The sensitivity of dependence of large scale flow characteristics in a four-level model atmosphere on a simulated planetary boundary layer

By J. W. SEARLE[1] and D. R. DAVIES, *University of Exeter, U.K.*

(Manuscript received February 2; revised version July 10, 1974)

ABSTRACT

A four-level, quasi-geostrophic, β plane, general circulation numerical model is developed, initially without a simulated boundary layer, and the sensitive dependence of large scale flow characteristics on the numerical choice of essential parameters (non-adiabatic heating fnnctions, static stability values, and internal turbulent stresses) is noted in a number of long period (100 day) integrations. It is particularly interesting to note that unless the values of turbulent stress coefficients are sufficiently large, the characteristic structures of cyclone waves and eddy kinetic energy functions are lost and these become random flow patterns and functions.

In order to obtain a lower limit estimate of the sensitivity of dependence of large scale flow model characteristics on the presence of a planetary boundary layer, a simple constant 'height' (from 1 000 to 900 mb) 'Ekman boundary layer' is then introduced, an analytic solution of the linearised boundary layer equations being matched to the numerical model through the vertical velocity field at the model grid points. The effect of this introduction on the structure of the meridional circulation is very marked, and the magnitude of this circulation is seen to depend quite sharply on the numerical value chosen for the model boundary layer eddy viscosity. It is also found that the most realistic large scale flow characteristics are reproduced with a boundary layer present, when the free atmosphere turbulence (vertical) stress coefficients are reduced to quite small values.

1. Introduction

Some of the recently constructed numerical models of the atmosphere's general circulation by large research institutions are becoming increasingly complex, with not only very high resolution systems but also highly detailed parameterisations of the observed physical processes. Such models are necessary and important tools in the developing study of meteorological problems, but it has also been shown that an improved understanding of certain aspects of large scale characteristics of the general circulation can be obtained through the use of relatively simple models. These are far less demanding in man power and computer requirements and time, the basic philosophy being that detailed accuracy in simulating observed phenomena is not necessary in a model used for the initial testing of parameterisations of particular features, as long as the large scale general characteristics of the circulation are reasonably well simulated.

In this paper a four-level, quasi-geostrophic, β plane, general circulation model is first developed from that used by Everson & Davies (1970). From some studies of recent observed climatological data, numerical values of (i) non-adiabatic heating functions, (ii) static stabilities, (iii) coefficients of turbulent (vertical) stresses, are chosen as fixed functions of geographical position, so that the model in long period integrations displays variations in the eddy kinetic energy function and cyclone wave flow patterns which are roughly characteristic of large scale observed dynamics. This is achieved initially without the inclusion of a simulated boundary layer and the sensitive dependence of large scale flow characteristics on the numerical choice of essential parameters

[1] Now at the British Ship Research Association, Wallsend-upon-Tyne, U.K.

is noted. Then in order to obtain a lower limit estimate of the dependence of large scale characteristics on the planetary boundary layer, a simple constant thickness 'Ekman' type boundary layer is introduced, an analytic solution of the linearised boundary layer equations being matched to the numerical model through the vertical velocity field at the model grid points.

2. The basic model

The model is similar in mathematical and geometrical construction to the two-level model of Everson & Davies (1970) which is based on that of Phillips (1956). Following the simple model philosophy, the atmosphere is assumed to be quasi-geostrophic in extra tropical latitudes, and at the end of each time step, the geostrophic equation is used to filter out gravity wave solutions from the primitive equations. This enables large time steps to be made in the numerical time integration scheme, so that long, 100 day, forecasts may be obtained relatively quickly.

The vertical resolution has been increased so that vertical variation in the thermal structure of the atmosphere may be included, and the vertical transfer of momentum may be studied in greater detail than is possible with a two-level model and a better test achieved of the effect of inserting a continuous boundary layer. Thermal energy is supplied to the model through a thermodynamic equation, defined at three levels equally spaced between the 'top and bottom' of the model atmosphere; these are assumed to be at 0 mb and 1 000 mb respectively. The non-adiabatic heating source is assumed constant in time, but has a latitudinal and height variation based on observed heating sources of net radiation, condensation heating and boundary layer heating (Newell et al., 1970). The three heating functions are shown in Fig. 1. The vertical thermal structure is characterised by three domain mean constant static stability parameters, estimated from temperature data given by Oort & Rasmussen (1971).

The domain of spatial integration is a β plane representation of a hemispherical surface, in which tropical and polar regions are included in order to provide available potential energy

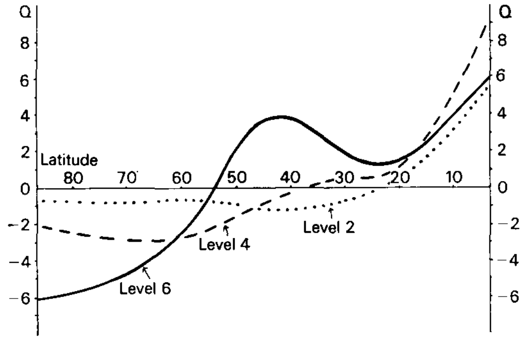

Fig. 1. Non-adiabatic heating functions Q at levels 2, 4 and 6, in J kg^{-1} sec^{-1} units, as functions of latitude. ——, level 6; --- level 4; .... level 2.

to organise a flow, through positive correlation of non-adiabatic heating and variation in temperature, about its value at the initial state of the model atmosphere. The dissipation mechanisms included are simple parameterisations of surface drag, and internal (vertical) eddy shearing stresses due to 'free atmosphere' turbulence, and also of sub-grid scale lateral 'diffusive' eddy stresses. No thermal vertical eddy transfer effects are included, to be consistent with the assumption of a constant static-stability.

A two-parameter prediction scheme is used, defined by the geostrophic stream function, ψ, and the relative potential vorticity function, q. The prognostic equation is given by (1) and the diagnostic equation by (2), with a notation as used by Phillips (1956):

$$\frac{\partial}{\partial t} q_l = -V_l \cdot \nabla(\beta y + q_l) + A\nabla^2 q_l - \frac{2R}{f_0 C_p} \times \left[\frac{\lambda_{l+1}^2}{(l+1)} Q_{l+1} - \frac{\lambda_{l-1}^2}{(l-1)} Q_{l-1}\right] - k_{l+1}(\zeta_l - \zeta_{l+2}) + k_{l-1}(\zeta_{l-2} - \zeta_l), \quad (1)$$

$$q_l = \zeta_l + \lambda_{l-1}^2(\psi_{l-2} - \psi_l) - \lambda_{l+1}^2(\psi_l - \psi_{l+2}), \quad (2)$$

where $l = 1, 3, 5, 7$, denotes the model momentum levels, 7 being the lower lever, λ_l is a measure of static stability, $\lambda_0 = \lambda_8 = 0$, and k_l is an internal turbulent (vertical) stress coefficient (as in Phillips, 1956).

Horizontal centered finite differences are used for the numerical approximation of the space derivatives, the resolution being 375 km.

Square grids are used, on a mesh covering a domain about 10 000 km north to south and 9 000 km east to west. The centered difference, 'leap-frog' scheme is used for the time integration, a forward time step being used for initialisation, and appropriate restarts. Computational stability is maintained by the use, in eq. (1), of implicit time averaging in the terms which are linear in q, and by the use of an 'Arakawa' type difference scheme applied to the non-linear advection terms. Horizontal Laplacian type terms, $A\nabla^2 q$, are included to represent subgrid scale lateral eddy diffusion and also to suppress high frequency waves arising out of round-off error at grid-points in the calculation. The Courant–Friedrichs–Lewy criterion allowed the convenient time-step of 30 minutes, with the above resolution.

Following Phillips (1956), the numerical forecast was made in two stages. In the first stage, the equations are limited to their zonal means, the integration of these 1-dimensional equations being very rapid and stable. The equations are initialised from an atmosphere at rest, with its isobaric and isentropic surfaces parallel and horizontal to the β-plane surface. The equations are maintained in the zonal flow state until a baroclinically unstable, by linear perturbation theory, horizontal temperature gradient has been established, at which time eddies, stimulated by a random number generator, are introduced into the mean flow system. The equations are then allowed their full variability to organizse a flow, under the imposed forcing functions.

The numerical experiments with the model and most of the model development, were made using the I.B.M 360/195 computer of the R.H.E.L., Harwell, U.K., and required about 25 minutes C.P.U. time to simulate and diagnose 100 days flow data, using a FORTRAN double-precision forecast code.

3. Parameterisation coefficient values and thermal behaviour of the model

The choice of 'optimum' numerical values for coefficients appearing in parameterisations of physical processes poses a very large problem in the running of any numerical model atmosphere. The interpretation of such a value in a physical sense, is also difficult. An 'optimum' value in our sense, is one that allows the model to simulate the main characteristic structure of the large scale dynamics, when given these values. Such values, which are usually representative of vast domain areas, cannot be deduced exactly from observed atmospheric data. However, an order of magnitude value can be found from observed data, and an optimum value for a *given model* has then to be found from numerical experiment. In the model described here, numerical values were required for the heating functions, the static-stability parameters, and the frictional dissipation parameters. The latter are discussed in section (5).

The thermal coefficients were based on available analyses of observational data, but they were also required to satisfy the mathematical constraint condition, i.e. that the domain integrated heating had to vanish at each model level. Great difficulty was experienced in model development in simulating a temperature distribution which was in reasonable agreement with observational data; this was not in fact achieved until optimum model values for the heating function and static-stability parameters were found by numerical experiment. It is interesting to note that the model was found to be particularly sensitive to the domain mean static-stability values, especially the lowest level value.

The experiments carried out to find model optimum parameter coefficient values do, however, illustrate the roles of the two primary large scale dynamical factors involved in maintaining the thermodynamic energy budget of the model. The latitudinal variation in non-adiabatic heating is of prime importance in creating a meridional temperature gradient between the simulated tropical and polar regions; this gradient, when it is sufficiently large, induces baroclinic instability in the flow system. Once the mid-latitude waves start amplifying, vertical motions become significant and meridional circulation developes. The amplifying eddies transport tropical heat polewards, and upwards; and the static-stability values are found in the model to be critical in controlling the thermal energy budget through the magnitude of the balancing meridional heat transports. The 'optimum' values of the heating functions which produced a physically reasonable 100 day integration are given in Fig. 1, the associated static-stability values being $\lambda_2 = 1.0$, $\lambda_4 = 8.0$, $\lambda_6 = 10.0$ respectively in units of 10^{-12} m^{-2}; we note that the equivalent value in Phillips' (1956) original β-plane model was $\lambda_4 = 1.5 \times 10^{-12}$ m^{-2}.

The atmospheric boundary layer parameterisation, and coefficients used in it, were investigated using the above numerical values for the basic thermal parameter coefficients. The values used for the vertical eddy shearing stresses and surface drag coefficients were empirical, but interesting results concerning the importance of these values were revealed by the results of the boundary layer experiments. The lateral eddy "diffusion" coefficient, A, was given the model optimum value of $A = 10^5$ m^2 sec^{-1} throughout.

4. The boundary layer parameterisation

Everson & Davies (1972), have recently discussed the possible physical limitations of using discrete level sampling points to represent boundary layer turbulence, as used for example by Delsol et al. (1971). It was pointed out that an analytic solution for the velocity profile in the boundary layer was better able to take into account all scales of turbulence from the tiny surface eddies upwards. Recently, Deardorff (1972) has proposed some complex analytic expressions for the velocity and temperature profiles in both the constant flux layer and the 'Ekman' layer. However, maintaining the simple model philosophy, it may be beneficial to investigate the effect in a model, of a simple analytic solution, before attempting to use a more complex system. The real atmospheric boundary layer is observed to vary widely in height and physical structure, but it is felt that an 'Ekman' layer of about 1 km depth or 100 mb thickness is a reasonable representative system to take initially to form a 'lower bound' estimate of the sensitivity of large scale flow dependence on the boundary layer.

We note that the introduction of this layer leads, in the numerical experiments where this is done, to a *continuously* varying vertical transfer of momentum through a *finite* depth of the model atmosphere. In other experiments the simpler approximation of earlier, Phillips type, general circulation models was adopted in which the frictional effects of this finite layer are contracted into a zero thickness surface condition. The dynamical processes in the very important lower 100 mb are then represented in very different ways in the two types of model, and the consequences of the difference are investigated in the numerical experiments described in section 5 of this paper.

A solution for the wind field in an incompressible constant height boundary layer, in which the eddy viscosity coefficient is assumed constant, is obtained in a similar manner to that of Everson & Davies (1972). However, their time dependent solution is discarded, as its analysis requires the eddy viscosity coefficient to vanish at the top of the boundary layer; this is physically inconsistent with non-zero values above this level, representing 'free air turbulence'. Also physically it seems at this stage better to simply extrapolate the numerical model dynamics of the two lowest levels down through the 900 mb–1 000 mb surface layer.

An analytic solution for the wind velocity as a function of height is easily obtained by integration of equations of motion representative of an 'Ekman' layer, in which advection is neglected. An 'austausch' type process, $\tau = -K(dV/dz)$, is used to represent the vertical transfer of momentum by the eddy shearing stresses, τ. As boundary conditions, the basic model surface drag parameterisation, following Phillips (1956), is used at the lower boundary of 1 000 mb, itself assumed co-incident with height $z = 0$. The wind field at the top of the boundary layer at height $z = h$, assumed coincident with the 900 mb surface, is assumed to be the quasi-geostrophic wind field of the numerical model, at that level. Integration of the continuity equation through the boundary layer, assuming the vertical motion vanishes on $z = 0$, leads to an approximate expression for the vertical motion, expressed as rate of change of pressure, at height h,

$$\omega(h) = -\frac{g\varrho}{2a}\sin(\alpha-\beta)\zeta_g \qquad (3)$$

where $a^2 = f_0/2K$, K = eddy viscosity coefficient for momentum in the boundary layer, α = angle which the surface wind and the surface wind shear subtend with the x-axis, β = angle which the geostrophic wind at $z = h$, subtends with the x-axis, and ζ_g = extrapolated geostrophic vorticity of the numerical model, at height h. This expression (3) may be used to replace the basic model's lower boundary value of a vanishing vertical motion, thus linking the analytic boundary layer solution to the numerical model.

In the numerical model, vertical symmetry (found to be convenient in our computation) is maintained by redistributing the model isobaric surfaces at 200 mb intervals between 100 mb and 900 mb, as opposed to the basic model distribution at 250 mb intervals between 0 mb and 1 000 mb.

Everson & Davies (1972) took the approximate value for the boundary layer eddy viscosity coefficient to be $K = 1$ m^2 sec^{-1}. This latter value is somewhat small and is more representative of the constant flux layer than that of an 'Ekman' layer of 100 mb depth. This value, however, did lead them to deduce a value of 26° for the geostrophic angle $(\alpha - \beta)$, which is certainly of the generally accepted order. Using a similar analysis to that applied by Everson & Davies (1972), the angle $(\alpha - \beta)$ is found to satisfy the equation

$$2Ka \sin(\alpha - \beta) = 0.5c\,|U_g|\,\{1 - \sin 2(\alpha - \beta)\}^{\frac{1}{2}} \quad (4)$$

where c is the surface drag parameter and $|U_g|$ is the surface geostrophic wind speed. If the top of the boundary layer at the height h, is that height at which the boundary layer wind field and the geostrophic wind field become parallel, then it may be shown that (as in Everson & Davies, 1972)

$$h = \frac{1}{a}\left(\frac{3\pi}{4} + \alpha - \beta\right). \quad (5)$$

If h is fixed at 100 mb or approximately 1 km above the surface, then (4) and (5) are simultaneous equations for K and $(\alpha - \beta)$. Assuming $c = 0.003$ and $|U_g| = 11$ m sec^{-1}, following Phillips (1956), these equations are found to have an approximate numerical solution giving $(\alpha - \beta) = 17°$ and $K = 7$ m^2 sec^{-1}, or $\varrho K = 8.4$ kg m^{-1} sec^{-1}, if the air density is assumed to be $\varrho = 1.2$ kg m^{-3}. The value of $\varrho K = 8.4$ kg m^{-1} sec^{-1} for the eddy viscosity coefficient, is in reasonable agreement with some observed data for the 'Ekman' layer, given by Priestley (1959).

Numerical experiments were carried out using both the above values of ϱK for the boundary layer eddy viscosity coefficient, in conjunction with experiments using a wide range of numerical values for 'free air turbulence' eddy viscosity coefficients of the numerical model.

5. Numerical experiments concerning vertical eddy stresses in the model

There appears to be no accepted definition of the concept of 'free air turbulence', and its representation in a grid scale model is therefore difficult. In this model, it is represented as a large scale 'austausch' process, with a constant eddy viscosity coefficient, whose physical interpretation may be regarded as representing all scales of turbulence up to the grid scale, and averaged over the grid squares. Kurihara (1972) has suggested that the numerical choice of eddy viscosity coefficients needs to be very precise, in weather prediction, and the experiments described here certainly support this finding.

Rossby & Montgomery (1935) suggested that above a certain height, the boundary layer eddy viscosity coefficient, ϱK, decreases linearly with height to a free air turbulence value of 5 kg m^{-1} sec^{-1}. The basic model coefficient values (before introducing a boundary layer) were first based on the assumption of this value for ϱK at 500 mb. Above this level ϱK was assumed zero, and a value for the level at 750 mb of $\varrho K = 11.4$ kg m^{-1} sec^{-1} was taken by linear interpolation between the value at 500 mb, and a value given by Priestley (1959) at the top of the constant flux layer, of $\varrho K = 18$ kg m^{-1} sec^{-1}. It is noted that the value of $\varrho K = 11.4$ kg m^{-1} sec^{-1} is larger than the estimated value of $\varrho K = 8.4$ kg m^{-1} sec^{-1} in an Ekman layer 100 mb deep. In reality atmospheric turbulence varies greatly in space and time, but we use these values to form a working hypothesis on which the basic model is constructed and we then note the effect of varying these parameters in the model. If the generally accepted notion that the eddy viscosity decreases with height above the constant flux layer is extended

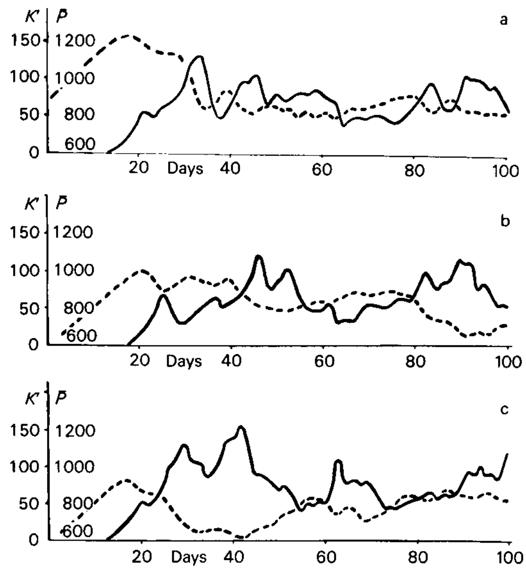

Fig. 2. Zonal mean available potential energy function P, and eddy kinetic energy function K', compared for numerical experiments E-1, E-2 and E-3, in J kg^{-1} units. ---, $\bar{P}$; ——, K'. Basic general ciculation model (GCM): 1 000 mb $\geqslant p \geqslant$ 0 mb. Boundary layer general circulation model (BLM): 900 mb $\geqslant p \geqslant$ 100 mb. Internal eddy stresses are $\varrho K = 5.0$ kg m^{-1} sec^{-1} at 500 mb, and $\varrho K = 11.4$ kg m^{-1} sec^{-1} at 750 mb, for all three experiments (700 mb for BLM). (*a*) E-1: GCM. (*b*) E-2: BLM; boundary layer eddy viscosity — $\varrho K = 8.4$ kg m^{-1} sec^{-1}. (*c*) E-3: BLM; boundary layer eddy viscosity — $\varrho K = 1.0$ kg m^{-1} sec^{-1}.

into the free atmosphere, then the basic model free air turbulence eddy viscosity coefficients are inconsistently too large, as compared with observed Ekman layer values. This illustrates the difficulty in interpreting the meaning of the free air turbulence coefficients. It could be argued that length and time scale averages should be considered in the free atmosphere part of the numerical model, differing markedly from those observed in the boundary layer and allowing for turbulent fluxes that increase in scale continuously from the tiny surface eddies upwards to various heights in the free atmosphere. The problem is further complicated by the fact that these eddy viscosity terms, together with the surface drag term, also play a large part in the computational stability maintaining (implicit averaging) scheme.

The numerical results of the experiments summarised below (discussed in detail by Searle, 1973), shed some insight into these problems. The experiments are denoted by E-n ($n = 1, 2, ..., 10$) for identification, E-1 being the first model experiment with parameter coefficient values given as above, with no boundary layer included, apart from the simple surface drag representation of Phillips (1956). Results from these experiments are illustrated by plotting two of the principal energy functions against time, the available potential energy of the zonal mean flow, $\bar{P}$, and the kinetic energy of the large scale eddies, K', being chosen for this purpose.

Fig. 2 compares the first three experiments: E-1 is the first basic model, and in E-2 and E-3 the same free air turbulence coefficient values are used, but the boundary layer parameterisation of section (4) is included in the model. In E-2 we use $\varrho K = 8.4$ kg m^{-1} sec^{-1}, and in E-3, we use $\varrho K = 1.0$ kg m^{-1} sec^{-2} in the boundary layer. It is interesting to note that in E-1, after the initial linear increase in $\bar{P}$, the value of $\bar{P}$ falls and does not again attain its first maximum value. This, however, did not occur in E-2 and in E-3 when the boundary layer was present. In E-2 and E-3, $\bar{P}$ regained the value of its first maximum later in the forecast. This results in less energy transfer to the eddies and so ultimately less to the kinetic energy of the zonal mean flow, $\bar{K}$. The $\bar{K}$ function then did not exhibit the anomalously high value around day 30 in E-2 and E-3, which is displayed in E-1.

It is also noticed that the generally accepted features of a baroclinic index cycle in these global energy functions are affected little by the introduction of the boundary layer. Typical baroclinic index cycle features, by which E-1 was deemed a satisfactory working model, are repeated with broad scale maxima and minima in the eddy kinetic energy, associated with variations in intensity of the meridional temperature gradient.

The presence of the boundary layer parameterisation was most noticeable in the model meridional circulation. As shown by Fig. 3, the lower dominant branches of the three cell circulation were in E-1 at level-7, but with the introduction of the boundary layer, the circulation at this level became indefinite, the lower dominant three branch structure descending into the boundary layer regions itself. The upper dominant three branches remained at level-3 for all the experiments. This gross effect was the same for E-2 and E-3 and was thus independent of the boundary layer eddy viscosity coefficient value, but the magnitudes of the wind speeds were higher for the higher value of this coefficient. Also a comparison of the energy dissipation functions showed these to be much the same for the three experiments. In this way these three experiments showed directly the influence of the boundary layer parameterisation of section (4), on the basic model which did not contain a boundary layer. The next set of experiments E-4, E-5 and E-6, were designed to investigate the effect of taking different fre air tnrbulence eddy viscosity coefficients in the first basic model.

Some data given by Priestley (1959) for the boundary layer eddy viscosity coefficient suggest that the value of $\varrho K = 5.0$ kg m^{-1} sec^{-2}, Rossby and Montgomery's free air turbulence value, occurs as low as 900 mb. It may thus be physically unrealistic to extend the friction layer into the great depths of the atmosphere. Experiments were then carried out in which the Rossby and Montgomery value was assumed at both 500 mb and at 750 mb, as in E-4, and in E-5 the value was included at 750 mb with a zero value at 500 mb; in E-6 a zero value was included at both 750 mb and 500 mb, so that there were no 'vertical' eddy stresses present at all. The energy functions $\bar{P}$ and K' of E-4, E-5 and E-6, are compared in Fig. 4, no boundary layer representation being included in E-4, 5, 6.

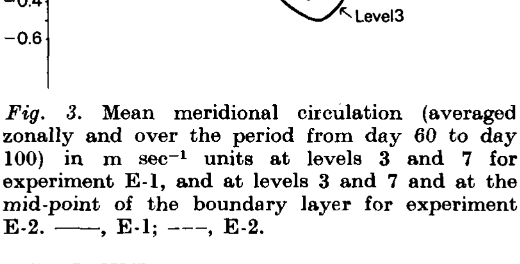

Fig. 3. Mean meridional circulation (averaged zonally and over the period from day 60 to day 100) in m sec^{-1} units at levels 3 and 7 for experiment E-1, and at levels 3 and 7 and at the mid-point of the boundary layer for experiment E-2. ——, E-1; ---, E-2.

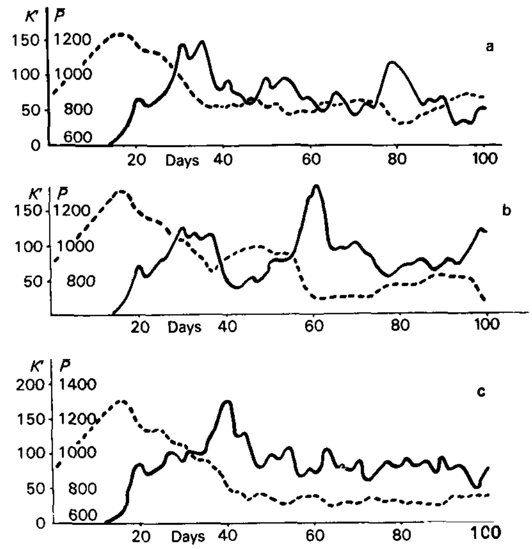

Fig. 4. Zonal mean available potential energy function $\bar{P}$, and eddy kinetic energy function K', compared for numerical experiments E-4, E-5 and E-6, in J kg^{-1} units. ---, $\bar{P}$; ——, K'. Basic general circulation model (GCM): 1 000 mb $\geqslant p \geqslant 0$ mb. (*a*) E-4: GCM; internal eddy stresses are $\varrho K = 5.0$ kg m^{-1} sec^{-1} at both 500 mb and 750 mb. (*b*) E-5; GCM; internal eddy stresses are $\varrho K = 0.0$ at 500 mb and $\varrho K = 5.0$ kg m^{-1} sec^{-1} at 750 mb. (*c*) E-6: GCM; internal eddy stresses are $\varrho K = 0.0$ at both 500 mb and 750 mb.

It is interesting to note that after the initialisation period, the eddy energy of E-6 is markedly random in time variation, whereas E-4 and E-5 retain the baroclinic index cycle features. This suggests that the degree of large scale mean vertical transfer of momentum is indeed very important in the model in organising the flow into the typical baroclinic index cycle pattern; this shows that choice of numerical values for the internal turbulence stress coefficient is very important.

No difficulty was experienced with the numerics in E-6, the numerical prediction scheme remaining stable despite the lack of the internal frictional smoothing terms. The surface drag term was found to be sufficient on its own, to maintain the computational stability.

It is also interesting to note that the eddy stress terms in these experiments were much smaller in their actions as energy dissipation mechanisms than in E-1; this is clearly a direct result of the use of smaller numerical values for the coefficients; their effects on

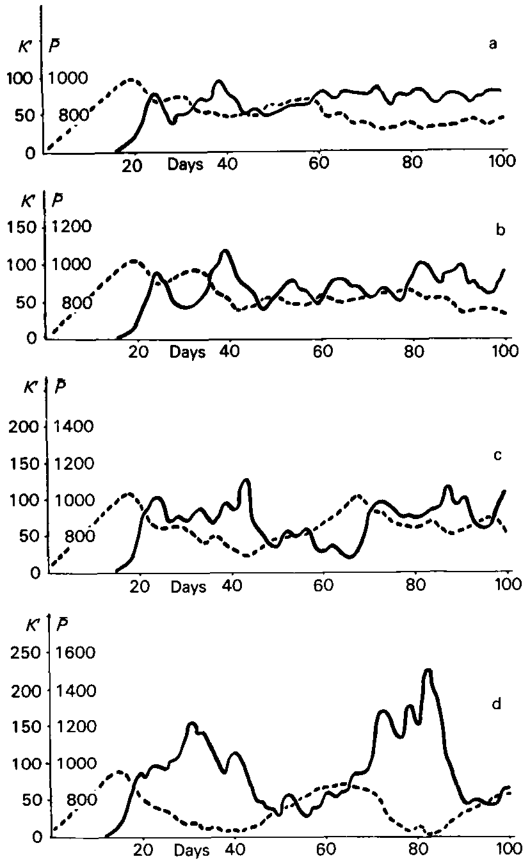

Fig. 5. Zonal mean available potential energy function $\bar{P}$, and eddy kinetic energy function K', compared for numerical experiments E-7, E-8, E-9 and E-10, in J kg^{-1} units. ---, $\bar{P}$; ——, K'. Boundary layer general circulation model (BLM): 900 mb $\geqslant p \geqslant$ 100 mb. (*a*) E-7: BLM; internal eddy stresses are $\varrho K = 5.0$ kg m^{-1} sec^{-1} at 500 mb and $\varrho K = 5.0$ kg m^{-1} sec^{-1} at 700 mb; boundary layer eddy viscosity is $\varrho K = 8.4$ kg m^{-1} sec $^{-1}$. (*b*) E-8: BLM; internal eddy stresses are $\varrho K = 0$ at 500 mb and $\varrho K = 5.0$ kg m^{-1} sec^{-1} at 700 mb; boundary layer eddy viscosity is $\varrho K = 8.4$ kg m^{-1} sec^{-1}. (*c*) *E*-9: BLM; internal eddy stresses are $\varrho K = 0$ at both 500 mb and 700 mb; boundary layer eddy viscosity it $\varrho K = 8.4$ kg m^{-1} sec^{-1}. (*d*) E-10: BLM; internal eddy stresses are $\varrho K = 0$ at both 500 mb and 700 mb; boundary layer eddy viscosity is $\varrho K = 1.0$ kg m^{-1} sec^{-1}.

dissipation were negligible compared with the dissipation by the sub-grid scale lateral eddies. The latter represent probably one of the least understood phenomena in geophysical scale meteorology. The simple parameterisation used in this model, as expressed in the A coefficient, was included primarily for numerical reasons, as a low pass filter; little physical significance can be attached to this result.

It was noticeable that in E-5, the ratio of mean to eddy kinetic energy ($\bar{K}/K'$), was nearer the real atmosphere's observed values than it was in E-4, where the internal stress value was included at 500 mb. The experiment E-5 also produced the best defined three cell meridional circulation of the set of three experiments. Consideration of these experiments together with the results of the basic model suggests that if there is to be a mean momentum transfer through the 500 mb surface in the model atmosphere, then the appropriate eddy viscosity value is very much smaller than that needed at 750 mb. The model certainly requires the inclusion of some representation of the friction layer, in order to secure model transfer of momentum downwards, and so to simulate a well defined baroclinic index cycle.

The experiments E-4, E-5 and E-6, were then repeated, but with the boundary layer parameterisation of section (4) included. The eddy viscosity coefficient value in the boundary layer was taken as $\varrho K = 8.4$ kg m^{-1} sec^{-2} in E-7, E-8 and E-9, the value $\varrho K = 1.0$ kg m^{-1} sec^{-2} being used in E-10. Experiments E-7 and E-8 correspond to E-4 and E-5 respectively, and E-9 and E-10 to E-6. The energy functions, K' and $\bar{P}$, for these last four experiments, are compared in Fig. 5.

It is immediately noticeable from E-8 and E-10, that baroclinic index cycle properties return to the flow, with the introduction of the continuous boundary layer solution, without the presence of any free air turbulence momentum transfer mechanisms. The K' oscillation in E-7 is considerably damped, especially after day 40, compared to those in E-9 and E-10. Also the oscillations in $\bar{P}$ with time are much more pronounced in E-9 and E-10, and the K' to $\bar{K}$ ratio is noted to be smaller when the internal stresses are present. As in the first experiment with the boundary layer parameterisation included, the gross effect on the meridional circulation was the same, but the magnitude of the circulation increased significantly in the mid-latitudes with the introduction of the free air internal stresses. Priestley (1967), has in fact suggested that the meridional circulation of the atmosphere is frictionally driven, and certainly the inclusion of a frictional boundary layer and also free air stresses, has a very marked effect on the intensity and structure of the meridional circulation of the model.

6. Conclusions

(i) The reaction of the model to the analytic boundary layer solution component is very marked. The meridional circulation is affected quite significantly by the inclusion of this parameterisation and by the numerical values chosen for the free air turbulence stresses. It would be of interest to carry out similar experiments with a primitive equation model.

(ii) The inclusion of this boundary layer simulation substantially alters the role of the model free air turbulence stresses in obtaining a typical baroclinic index cycle in the forecast flow.

(iii) In a model which does not include a finite thickness boundary layer, appreciable 'internal' stress values are found to be necessary to obtain the typical large scale flow pattern, but with the continuous Ekman layer included, these internal stresses appear to be no longer necessary.

Acknowledgement

J. W. Searle gratefully acknowledges the financial aid of a N.E.R.C., U.K., Research Studentship.

REFERENCES

Deardorff, J. W. 1972. Parameterisation of the planetary boundary layer for use in general circulation models. *Mon. Wea. Rev. 100*, 93–106.

Delsol, F. Miyakoda, K. and Clarke, R. H. 1971. Parameterized process in the surface boundary layer of an atmospheric circulation model. *Q. J. R. Met. Soc. 97.* 181–209.

Everson, P. J. and Davies, D. R. 1970. On the use of a simple two-level model in general circulation studies. *Q. J. R. Met. Soc. 96*, 404–412.

Everson, P. J. and Davies, D. R. 1972. Ekman boundary layer interaction in a numerical model of the general circulation. *Q. J. R. Met. Soc. 98*, 412–419.

Kurihara, Y. 1972. Experiments on the seasonal variation of the general circulation in a statistical dynamic model. *J. Atmospheric Science 30*, 25–49.

Newell, R. E., Vincent, D. G., Dopplick, T. G., Ferruzza, D. & Kidson, J. W. 1970. The energy balance of the global atmosphere. In *The global circulation of the atmosphere* (ed. G. A. Corby), pp. 42–91.

Oort, C. H. B & Rasmussen, E. M. 1971. Atmospheric circulation statistics. U.S. Department of Commerce, N.O.A.A., Professional Paper 5.

Phillips, N. A. 1956. The general circulation of the atmosphere; a numerical experiment. *Q. J. R. Met. Soc. 82*, 123–164.

Priestley, C. H. B. 1959. Turbulent transfer in the lower atmosphere, pp. 1–130. University of Chicago Press.

Priestley, C. H. B. 1967. Handover in scale of the fluxes of momentum, heat etc. in the atmospheric boundary layer. *J. Physics. of Fluids 10*, No. 9, Part 2, 38–46.

Rossby C. G. & Montgomery, R. B. 1935. The layer of frictional influence in wind and ocean currents. Papers in Physical Oceanography and Meteorology, M.I.T. and Woods Hole Oceanographic Institutions, vol. 3, No. 3.

Searle, J. W. 1973. Boundary layer parameterisation in a four level model atmosphere. Ph.D. Thesis, University of Exeter, U.K.

ЧУВСТВИТЕЛЬНОСТЬ ЗАВИСИМОСТИ ХАРАКТЕРИСТИК КРУПНОМАСШТАБНОГО ПОТОКА В ЧЕТЫРЕХУРОВЕННОЙ МОДЕЛИ АТМОСФЕРЫ ОТ ПЛАНЕТАРНОГО ПОГРАНИЧНОГО СЛОЯ

Построена четырехуровенная, квазигеострофическая численная модель общей циркуляции на β-плоскости сначала без модельного пограничного слоя. Чувствительность зависимости характеристик крупномасштабного течения от величин существенных параметров (неадиабатического нагревания, статической устойчивости, внутренних турбулентных напряжений) определяется для ряда длительных (100 дней) интегрирований. Особенно интересно отметить, что, пока величины коэффициентов турбулентного напряжения не взяты достаточно большими, характерная структура циклонических волн и вихревой кинетической энергии теряется, и последние становятся случайными полями и функциями. Для получения нижней оценки чувствительности зависимости характеристик

модели крупномасштабного потока от присутствия планетарного пограничного слоя вводился простейший «пограничный слой Экмана» с постоянной «высотой» (от 1 000 до 900 *мб*). При этом аналитическое решение линеаризированных уравнений пограничного слоя использовалось в численной модели через посредство вертикальной скорости в точках сетки модели. Эффект такого введения на структуру меридиональной циркуляции весьма значителен, и величина циркуляции очень сильно зависит от величины турбулентной вязкости, выбранной для модели пограничного слоя. Найдено также, что наиболее реалистические характеристики крупномасштабного потока воспроизводятся при введении пограничного слоя, когда коэффициенты напряжения вертикальной турбулентности в свободной атмосфере принимают весьма малые значения.